

# Hydrotris(triazolyl)borate Complexes as Functional Models for Cu Nitrite Reductase: The Electronic Influence of Distal Nitrogens

Mukesh Kumar,<sup>†,‡</sup> Natalie A. Dixon,<sup>†,‡</sup> Anna C. Merkle,<sup>§</sup> Matthias Zeller,<sup>#</sup> Nicolai Lehnert,<sup>\*,§</sup> and Elizabeth T. Papish<sup>\*,†</sup>

<sup>†</sup>Department of Chemistry, Drexel University, 3141 Chestnut Street, Philadelphia, Pennsylvania 19104, United States

<sup>§</sup>Department of Chemistry, University of Michigan, Ann Arbor, Michigan 48109, United States

<sup>#</sup>Department of Chemistry, Youngstown State University, 1 University Plaza, Youngstown, Ohio 44555, United States

## Supporting Information

**ABSTRACT:** Hydrotris(triazolyl)borate (Ttz) ligands form  $\text{CuNO}_x$  ( $x = 2, 3$ ) complexes for structural and functional models of copper nitrite reductase. These complexes have distinct properties relative to complexes of hydrotris(pyrazolyl)borate (Tp) and neutral tridentate N-donor ligands. The electron paramagnetic resonance spectra of five-coordinate copper complexes show rare nitrogen superhyperfine couplings with the Ttz ligand, indicating strong  $\sigma$  donation. The copper(I) nitrite complex  $[\text{PPN}]^+[(\text{Ttz}^{\text{tBu,Me}})\text{Cu}^{\text{I}}\text{NO}_2]^-$  has been synthesized and characterized and allows for the stoichiometric reduction of  $\text{NO}_2^-$  to NO with  $\text{H}^+$  addition. Anionic Cu(I) nitrite complexes are unusual and are stabilized here for the first time because Ttz is a good  $\pi$  acceptor.

Bacterial denitrification corresponds to the stepwise reduction of nitrate to dinitrogen and is an important part of the global nitrogen cycle, including the breakdown of excess fertilizers.<sup>1</sup> A key step in denitrification is nitrite reduction to NO as performed by copper nitrite reductase (CuNiR).<sup>1</sup> Note that NO generation and reduction processes are relevant to human health and how bacteria evade our immune response.<sup>2</sup> The active site in CuNiR contains a Cu ion ligated by three histidines (His) in a facial arrangement.<sup>1</sup> In the catalytic cycle, it is proposed that a four-coordinate  $\text{Cu}^{\text{II}}$ -aqua species binds nitrite and is reduced to  $\text{Cu}^{\text{I}}$  (Figure 1, L is the enzyme).<sup>3</sup> The resulting copper(I) nitrite complex can then reduce nitrite to form NO upon protonation. Many of these steps have been modeled previously with copper(I) nitrite complexes of tridentate N donors,<sup>4</sup> but our model is unique in three respects: (1) we are the first to use a *monoanionic* N-donor ligand; (2) consequently, ours is the first study to show

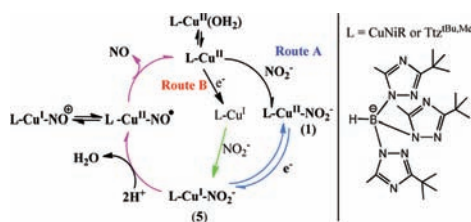


Figure 1. Key steps in enzymatic nitrite reduction by CuNiR.

nitrite reduction starting from an anionic copper(I) complex; (3) our model contains remote sites in the triazole rings for binding  $\text{H}^+$  and changing ligand donor properties in situ.<sup>5</sup> Hydrogen bonding is known to influence biological function, e.g. globins and peroxidases differ principally by H bonds.<sup>6</sup> For CuNiR, hydrogen bonds may stabilize unusual NO and  $\text{NO}_2^-$  binding modes.<sup>7</sup>

Surprisingly, monoanionic Tp ligands seem unable to stabilize  $[\text{LCu}^{\text{I}}(\text{NO}_2)]^-$  complexes<sup>4</sup> and thus have not been used as functional mimics for nitrite reduction to NO. However,  $\text{LCu}^{\text{I}}(\text{NO}_2)$  complexes have been isolated with sterically bulky *neutral* N donors as supporting ligands,<sup>8</sup> such as tris(1-pyrazolyl)methane (Tpm),<sup>3</sup> tris(4-imidazolyl)carbinol,<sup>3</sup> and 1,4,7-triazacyclononane (tacn) derivatives.<sup>4</sup> Hydrotris(triazolyl)borate (Ttz) ligands differ from Tp ligands in terms of  $\sigma$ -donor and  $\pi$ -acceptor capability, as is evident from differences in the  $\text{LCuCO}$  stretching frequencies [ $\nu(\text{CO})$  shifts from 2059 to 2080  $\text{cm}^{-1}$  as L changes from  $\text{Tp}^{\text{tBu,Me}}$  to  $\text{Ttz}^{\text{tBu,Me}}$ ].<sup>9</sup> Also, protonation at the four position N atom of one triazole ring in Ttz can reduce the donicity of the Ttz ligand, to reversibly alter the properties of this ligand in situ.<sup>5</sup>

Bulky hydrotris(3-*tert*-butyl-5-methyl-1,2,4-triazolyl)borate ( $\text{Ttz}^{\text{tBu,Me}}$ ) supports low-coordinate complexes with late-first-row transition metals.<sup>5,9</sup> In order to model CuNiR, we first explored how the change in the ligand from Tp to Ttz alters the structures and the spectral properties of stable  $\text{LCu}^{\text{II}}\text{NO}_x$  ( $x = 2, 3$ ) complexes. Nitrate and nitrite complexes of Ttz and Tp were synthesized by substitution of the chloride ligand in  $\text{LCuCl}$  ( $\text{L} = \text{Tp}^{\text{tBu,Me}}, \text{Ttz}^{\text{tBu,Me}}$ ) complexes previously reported.<sup>9,10</sup> The new complexes  $(\text{Ttz}^{\text{tBu,Me}})\text{CuNO}_2$  (**1**),  $(\text{Tp}^{\text{tBu,Me}})\text{CuNO}_2$  (**2**), and  $(\text{Ttz}^{\text{tBu,Me}})\text{CuNO}_3$  (**3**) were synthesized in 70, 66, and 67% yield, respectively, and characterized by elemental analysis, high-resolution mass spectrometry (HRMS), crystallography, and spectroscopy. All structures are five-coordinate, but there are distinct structural and electronic differences between analogous Ttz and Tp complexes (Figure 2, Supporting Information, SI).

Crystallography shows that **1** has a nearly symmetric bidentate  $\kappa^2$ -nitrite ligand [ $\text{Cu}-\text{O} = 2.008(2)$  and  $2.061(2)$  Å] in a distorted square-pyramidal ( $\text{sp}$ ) geometry ( $\tau = 0.375$ ; Figure 2a). This contrasts with **2**, which has an asymmetric

Received: January 21, 2012

Published: June 6, 2012

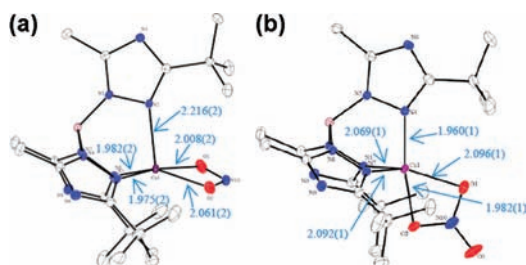


**Figure 2.** Molecular diagrams of (a) **1** and (b) **3**. H atoms and solvent (in **1**) are omitted for clarity. Bond distances (Å) to Cu shown in blue.

bidentate nitrite ligand [Cu–O = 1.973(2) and 2.255(3) Å] and a distorted trigonal-bipyramidal (tbp) copper ( $\tau = 0.751$ ; Figure S21 in the SI; the other unique molecule in the asymmetric unit is very similar). The structure of **2** is also similar to (Tp<sup>tBu,Pr</sup>)CuNO<sub>2</sub>.<sup>11</sup> **3** (Figure 2b) has an asymmetric bidentate nitrate [Cu–O = 2.096(1) and 1.982(1) Å; similar in nitrate binding to (Tp<sup>tBu,Me</sup>)CuNO<sub>3</sub>]<sup>12</sup> and shows a tbp distortion ( $\tau = 0.711$ ) in contrast to **1**. This differs from the bulky Tp and Tpm complexes of Cu(NO<sub>3</sub>) in the literature, which are perfectly sp [(Tp<sup>tBu</sup>)CuNO<sub>3</sub>,  $\tau = 0$ ],<sup>13</sup> distorted sp [(Tpm<sup>tBu,Me</sup>)CuNO<sub>3</sub>]<sup>+</sup>,  $\tau = 0.39$ – $0.10$ ), and between sp and tbp [(Tp<sup>tBu,Me</sup>)CuNO<sub>3</sub>,  $\tau = 0.55$  and  $0.48$ ].<sup>12</sup> It appears that these different geometries are very close in energy for these complexes, and a slight change in the sterics, electronics, or solvent can favor one form over the other. Thus, with Ttz<sup>tBu,Me</sup> and Cu<sup>II</sup>, nitrite favors sp and nitrate favors tbp in the solid state.

Electron paramagnetic resonance (EPR) spectroscopy was used to probe the electronic differences between Tp and Ttz complexes of copper(II). Figure 3 shows the experimental and simulated spectra for **3**, the nitrate complex; the inset shows that to obtain a satisfactory fit of the EPR spectrum, nitrogen superhyperfine (SH) splittings for the three coordinating triazole N atoms had to be included. Similarly, the EPR spectrum for **1**, the nitrite complex, shows the presence of SH couplings to three triazole N atoms (Figure S4 in the SI). While these spectra are overall similar in terms of *g* values and SH couplings, the lower quality of the fit in the nitrite complex and

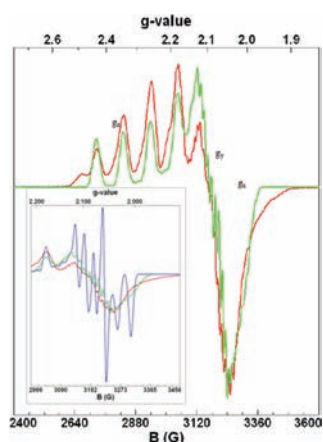


**Figure 3.** EPR spectrum of **3** at 77 K in frozen CH<sub>2</sub>Cl<sub>2</sub> (red) and fit (green). Fit parameters:  $g_z = 2.3$ ,  $g_y = 2.0855$ ,  $g_x = 2.0444$ . Hyperfine splittings:  $^{63}\text{Cu}A_z = 343$  MHz,  $^{63}\text{Cu}A_y = 80$  MHz,  $^{63}\text{Cu}A_x = 116$  MHz. SH coupling constants:  $^{14}\text{N}A_z = 25$  MHz,  $^{14}\text{N}A_y = 37$  MHz,  $^{14}\text{N}A_x = 46$  MHz. Inset: the fit without the N coupling (blue) is unsatisfactory.

the broad  $g_z$  region indicate the presence of other species in solution. Similar SH splittings have been observed from Cu to histidine N atoms in CuNiR using ENDOR (values of *A* to inequivalent N atoms are 37, 31, and 19 MHz), and thus our model reproduces key spectroscopic features of CuNiR.<sup>14</sup>

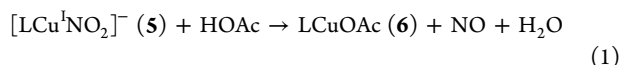
From the EPR fit, the N-atom SH coupling constants in **1** and **3** are estimated to range from 20 to 50 MHz. The observation of these features is remarkable because N-atom SH splittings are rarely observed in copper(II) complexes with pyrazole or related ligands.<sup>15</sup> For example, the EPR spectrum of the Tp analogue, **2**, does not show such SH couplings (Figure S6 in the SI). This finding provides direct experimental evidence that Ttz is generally a stronger  $\sigma$ -donating ligand than Tp. Importantly, the *g* values indicate that **1** and **3** have  $d_{z^2}$  ground states (due to  $g_z < g_x, g_y$ ) in the solid state (see Figures S5 and S3 in the SI); in contrast, **1** and **3** in a frozen solution both have  $d_{x^2-y^2}$  ground states ( $g_z > g_x, g_y$ ; see Figures 3 and S4 in the SI). This provides evidence that **1** and **3** have different geometries in solution and in the solid state.

The EPR spectrum of (Ttz<sup>tBu,Me</sup>)CuCl<sup>9</sup> (**4**; Figure S7 in the SI), is rhombic and similar to that of (Tp<sup>iPr2</sup>)CuCl.<sup>16</sup> Like the Tp complex, coupling to the triazole N atoms is not observed (resolved) in **4**. It appears that with Ttz the SH couplings to N atoms are only well resolved in the five-coordinate geometry. We have not observed SH couplings to Ttz N atoms in the EPR spectra of six-coordinate Mn-, Co-, and Cu<sup>II</sup>bis(Ttz) complexes.<sup>17</sup> Upon the addition of *N,N*-dimethylformamide (DMF) to **4**, the EPR spectrum (Figure S8 in the SI) becomes axial, indicating a change of the coordination number, with a  $d_{z^2-y^2}$  ground state. This is consistent with the formation of a DMF adduct (**4**<sub>DMF</sub>) that is presumably five-coordinate, similar to (Tp<sup>iPr2</sup>)CuCl.<sup>16</sup> Uniquely for **4**, a change in the geometry also leads to the appearance of the N-atom SH couplings.

A density functional theory (DFT) calculation on the electronic structure of **3** (using the crystal structure geometry) shows that the singly occupied molecular orbital (SOMO) of the complex has large contributions of Cu atoms (34% d), nitrate (32%), and triazole N atoms (29%); see Figure S11 in the SI. A similar calculation was performed on (Tp<sup>tBu,Me</sup>)CuNO<sub>3</sub>, using the same atomic coordinates, and in this case, an overall similar SOMO is obtained (Cu, 37% d; nitrate, 34%; pyrazoles, 21%). The key difference between these complexes is that the contribution of the triazole ligand to the SOMO is distinctively larger compared to pyrazole, indicating that Ttz is a somewhat stronger  $\sigma$  donor compared to the analogous Tp ligand (Table S3 in the SI). Thus, we propose that the coordinating N atoms in Ttz<sup>tBu,Me</sup> show larger SH coupling constants compared to those of Tp<sup>tBu,Me</sup>, allowing for the spectral resolution of the N-atom SH bands only in the Ttz<sup>tBu,Me</sup> complex.

To observe biomimetic nitrite reduction, we then prepared [(Ttz<sup>tBu,Me</sup>)Cu<sup>I</sup>(NO<sub>2</sub>)]<sup>−</sup> as a model of the reduced form of the enzyme with nitrite bound (Figure 1, **5**). This molecule is very air- and moisture-sensitive and was only cleanly isolated as the PPN<sup>+</sup> salt [PPN = bis(triphenylphosphine)iminium]. The treatment of Tl(Ttz<sup>tBu,Me</sup>) with Cu<sup>I</sup>Cl in CH<sub>2</sub>Cl<sub>2</sub> presumably produced [(Ttz<sup>tBu,Me</sup>)Cu]<sub>*n*</sub>, which was treated in situ with [PPN]<sup>+</sup>NO<sub>2</sub> to produce [PPN]<sup>+</sup>[(Ttz<sup>tBu,Me</sup>)Cu<sup>I</sup>NO<sub>2</sub>]<sup>−</sup> (**5**) in 65% yield. **5** was recrystallized from CH<sub>2</sub>Cl<sub>2</sub>/hexane and characterized by HRMS and <sup>1</sup>H and <sup>13</sup>C NMR and IR spectroscopy. The yellow color and the strong ( $\epsilon \sim 10^3$  M<sup>−1</sup> cm<sup>−1</sup>) metal-to-ligand charge-transfer bands at  $\lambda_{\text{max}} = 262$ – $275$  nm suggest an N-bound copper(I) nitrite.<sup>3</sup> Further evidence for a copper nitrite complex comes from the antisymmetric N–O stretch at

1078 cm<sup>-1</sup> [ $\nu_{\text{as}}(\text{N}-\text{O})$  shifts to 1060 cm<sup>-1</sup> with <sup>15</sup>N-labeled nitrite (Figure S18 in the SI)]. **5** reacts with acetic acid to mediate nitrite reduction (Figure 1, magenta arrows, and eq 1), and we have characterized both the Cu- and N-containing products of this reaction. When this reaction is run on a preparative scale with **5** and 2.4 equiv of acetic acid in CH<sub>2</sub>Cl<sub>2</sub>, the solution immediately turns bluish-green and (Ttz<sup>tBu,Me</sup>)-CuOAc (**6**) is isolated in 78% yield. This product was subsequently crystallographically and spectroscopically characterized (*taken directly from the nitrite reduction*). Complex **6** prepared via this route is identical (by UV-vis, IR, and MS) with samples prepared directly from copper(II) acetate (see the SI). The EPR spectrum of **6** shows a d<sub>x<sup>2</sup>-y<sup>2</sup></sub> ground state in both the solution and solid state (see Figures S9–10 in the SI). The preliminary crystallographic data of **6** (see the SI) show a sp Cu<sup>I</sup> ion.



Furthermore, NO(g) formation was confirmed by trapping and UV-vis detection with (TPP)Co (TPP<sup>2-</sup> = tetraphenylporphyrinato dianion) in CH<sub>2</sub>Cl<sub>2</sub> (Figure S20 in the SI). When **5** is in a separate vessel from (TPP)Co but gas can diffuse between the two vessels, the addition of acetic acid (2 equiv) to **5** produces (TPP)CoNO in 86–89% yield. The use of 4 equiv of HOAc increases the yield to 93% (see the SI). Thus, yields of NO from nitrite reduction are high despite the possibility of inefficient mixing of NO gas with the (TPP)Co solution, and this shows that the spectral changes can only be due to NO binding. In a control experiment, no NO was detected by UV-vis analysis of (TPP)Co when HOAc was added to [PPN]NO<sub>2</sub>; thus, our copper(I) complex is essential for NO generation.

Because Cu<sup>II</sup> reduction to Cu<sup>I</sup> is a key step in CuNiR catalysis (Figure 1), we were interested in measuring the potential for this process. The Cu<sup>I/II</sup> couple was observed starting from the copper(II) complex **1**, and the E<sub>1/2</sub> and E<sub>pc</sub> values measured by rotating disk electrode and cyclic voltammetry, respectively, were both -1.45 V versus a nonaqueous Ag/Ag(ClO<sub>4</sub>) reference electrode (APE; Figure S19 in the SI). This is significantly lower than the values of -0.20 to -0.03 V with neutral ligands in LCu<sup>I</sup>NO<sub>2</sub> complexes<sup>3</sup> (L = substituted tacn, Tim, Tpm; adjusted to be relative to APE). Thus, reduction (Cu<sup>II</sup> to Cu<sup>I</sup>) is less favorable with Ttz than with the above neutral ligands because an anionic complex (similar to **5**) forms. Presumably, one-electron reduction of (Tp<sup>R,R'</sup>)CuNO<sub>2</sub> complexes is even more disfavored or yields an unstable species;<sup>4</sup> this underscores the advantage of triazole-based ligands, which can stabilize anions by  $\pi$  back-bonding.

Thus, we have observed steps that are analogous to all of the colored arrows in Figure 1 because we (1) performed chemical synthesis (in green) to isolate **5** as a model of the reduced, nitrite-bound enzyme, (2) observed Cu<sup>I/II</sup> redox processes (in blue), and (3) observed nitrite reduction to NO (in magenta). It is not surprising that the Cu<sup>I/II</sup> reduction potential is much lower with **1** than with neutral tridentate ligands.<sup>3,18</sup> Therefore, nitrite reduction with **5** is novel considering suggestions that more accessible redox potentials lead to more efficient nitrite reduction.<sup>18</sup> Our work shows that if anionic copper(I) nitrite complexes can be accessed (e.g. **5**), nitrite reduction is fast and quantitative, in part because of a very negative reduction potential. Significantly, nitrite reduction can be accelerated with excess H<sup>+</sup> in our model, and Ttz ligands are the first monoanionic tripodal N donors to functionally mimic

CuNiR. The remote N atoms on the triazole rings provide an opportunity to fine-tune the properties and redox potentials of the complexes via hydrogen bonding or protonation,<sup>5</sup> and this may have mechanistic implications for nitrite reduction.

## ■ ASSOCIATED CONTENT

### 📄 Supporting Information

Crystallographic data (CIF format), further experimental details, EPR spectra, and DFT calculation results. This material is available free of charge via the Internet at <http://pubs.acs.org>.

## ■ AUTHOR INFORMATION

### ✉ Corresponding Author

\*E-mail: [lehnertn@umich.edu](mailto:lehnertn@umich.edu), [ep322@drexel.edu](mailto:ep322@drexel.edu).

### 👤 Author Contributions

‡The first two authors contributed equally to this work.

### 📄 Notes

The authors declare no competing financial interest.

## ■ ACKNOWLEDGMENTS

We thank D.U., NSF CAREER (CHE-0846383 to E.T.P.), 3M (NTFG 5286067 to N.L.) for kind financial support; T. Wade for MS; A. W. Addison, D. L. Tierney for discussions.

## ■ REFERENCES

- (1) Merkle, A. C.; Lehnert, N. *Dalton Trans.* **2012**, 3355.
- (2) Anjum, M. F.; Stevanin, T. M.; Read, R. C.; Moir, J. W. *J. Bacteriol.* **2002**, *184*, 2987.
- (3) Kujime, M.; Izumi, C.; Tomura, M.; Hada, M.; Fujii, H. *J. Am. Chem. Soc.* **2008**, *130*, 6088.
- (4) Halfen, J. A.; Mahapatra, S.; Wilkinson, E. C.; Gengenbach, A. J.; Young, V. G.; Que, L.; Tolman, W. B. *J. Am. Chem. Soc.* **1996**, *118*, 763.
- (5) Kumar, M.; Papish, E. T.; Zeller, M.; Hunter, A. D. *Dalton Trans.* **2011**, *40*, 7517.
- (6) Ozaki, S.; Roach, M. P.; Matsui, T.; Watanabe, Y. *Acc. Chem. Res.* **2001**, *34*, 818.
- (7) Antonyuk, S. V.; Strange, R. W.; Sawers, G.; Eady, R. R.; Hasnain, S. S. *Proc. Natl. Acad. Sci. U.S.A.* **2005**, *102*, 12041.
- (8) Yokoyama, H.; Yamaguchi, K.; Sugimoto, M.; Suzuki, S. *Eur. J. Inorg. Chem.* **2005**, *2005*, 1435.
- (9) (a) Papish, E. T.; Donahue, T. M.; Wells, K. R.; Yap, G. P. A. *Dalton Trans.* **2008**, 2923. (b) Bongiovanni, J. L.; Rowe, B. W.; Fadden, P. T.; Taylor, M. T.; Wells, K. R.; Kumar, M.; Papish, E. T.; Yap, G. P. A.; Zeller, M. *Inorg. Chim. Acta* **2010**, *363*, 2163. (c) Jernigan, F. E., III; Sieracki, N. A.; Taylor, M. T.; Jenkins, A. S.; Engel, S. E.; Rowe, B. W.; Jove, F. A.; Yap, G. P. A.; Papish, E. T.; Ferrence, G. M. *Inorg. Chem.* **2007**, *46*, 360.
- (10) Yoon, K.; Parkin, G. *Polyhedron* **1995**, *14*, 811.
- (11) Lehnert, N.; Cornelissen, U.; Neese, F.; Ono, T.; Noguchi, Y.; Okamoto, K.; Fujisawa, K. *Inorg. Chem.* **2007**, *46*, 3916.
- (12) Fujisawa, K.; Iwamoto, H.; Tobita, K.; Miyashita, Y.; Okamoto, K. *Inorg. Chim. Acta* **2009**, *362*, 4500.
- (13) Han, R.; Looney, A.; McNeill, K.; Parkin, G.; Rheingold, A. L.; Haggerty, B. S. *J. Inorg. Biochem.* **1993**, *49*, 105.
- (14) Veselov, A.; Olesen, K.; Sienkiewicz, A.; Shapleigh, J. P.; Scholes, C. P. *Biochemistry* **1998**, *37*, 6095.
- (15) Fujisawa, K.; Kanda, R.; Miyashita, Y.; Okamoto, K. *Polyhedron* **2008**, *27*, 1432.
- (16) Kitajima, N.; Fujisawa, K.; Moro-oka, Y. *J. Am. Chem. Soc.* **1990**, *112*, 3210.
- (17) Oseback, S. N.; Shim, S. W.; Kumar, M.; Greer, S. M.; Gardner, S. R.; Lemar, K. M.; DeGregory, P. R.; Papish, E. T.; Tierney, D. L.; Zeller, M.; Yap, G. P. A. *Dalton Trans.* **2012**, *41*, 2774.
- (18) Woollard-Shore, J. G.; Holland, J. P.; Jones, M. W.; Dilworth, J. R. *Dalton Trans.* **2010**, *39*, 1576.